Noble Metal Doped TiO_2 Thin Films In The Efficient Removal of Mordant Orange-1: Insights of Degradation Process

Chhakchhuak Vanlalhmingmawia
Mizoram University
Chhakchhuak Lalhriatpuia
Mizoram University Pachhunga University College
Diwakar Tiwari (diw_tiwari@yahoo.com)
Mizoram University https://orcid.org/0000-0002-9177-9704
Dong-Jin Kim
Hallym University

Research Article

Keywords: Insights of degradation, Kinetic Studies, Mineralization of Mordant Orange-1, Mordant Orange-1, Nanocomposite, Surface Plasmon Resonance.

Posted Date: September 2nd, 2021

DOI: https://doi.org/10.21203/rs.3.rs-661533/v1

Abstract

Nanocomposite Ag^0(NPs)/TiO_2 is synthesized in a facile template method enabling fine particles of reduced Ag evenly distributed within the titania network. The morphological studies of nanocomposite were extensively performed employing SEM/EDX (Scanning Electron Spectroscopy/Energy Dispersive X-ray), TEM (Transmission Electron Microscopy) and AFM (Atomic Force Microscopy). The newer insights in the photocatalytic elimination of Mordant Orange-1 (MO1) was obtained using the nanocomposite thin film for various parametric studies utilizing the UV-A and LED illuminations. The kinetics of degradation of MO1 was performed and the rate constant was favoured at lower concentrations of MO1. However, the elimination efficiency of MO1 was favoured with decrease in solution pH. The NPOC results inferred that fairly good extent of MO1 was mineralized using thin film catalyst for both the UV-A and LED illuminations. The minimal effect of several co-ions demonstrated applicability of thin films in the elimination of MO1 and the stability of the thin film has shown the potential applicability of thin film catalyst. Further, mechanism of photocatalytic degradation was demonstrated with the radical scavengers studies and ascertained the reaction pathways.

Introduction

The contamination of aquatic environments with innumerable dye compounds is a greater environmental concern. Several dyes, dye precursors are seemingly known as carcinogenic/mutagenic (Matouq et al. 2014). The main entry route of synthetic dyes in water bodies is through the effluent discharged from the industries *viz*., textile, paper, leather, paint, food, cosmetics, pharmaceuticals, hair colourings etc. (Verma et al. 2012; Papić et al. 2004). It was reported that the annual dye production exceeds 7 x 10^5 tons (Lee et al. 2006; Riera-Torres et al. 2010) and nearly 10–15% of the total dyes are directly entering through the effluents during the synthesis and dyeing processes (Husain 2006; Gupta and Suhas 2009; Hai et al. 2007). Moreover, textile dyes estimated around 2.8x10^5 tons are eventually released into the water bodies through the industrial effluents every year (Jin et al. 2007; H et al. 2017). Synthetic dyes are refractory in nature as they are trivially biodegradable in nature and are known to be highly stable against some oxidizing agents (Sadeghzade-Attar 2018). Hence, such dyes are often released from the current wastewater treatment plants and entered into the water bodies which caused serious adverse effects to the aquatic environment (Jung et al. 2016; Su et al. 2011; Muhd Julkapli et al. 2014). Azo dye compounds are known to be highly toxic causing several health issues such as allergy, skin diseases, cancer, defect in embryo development, etc. (Rosu et al. 2017; Alves de Lima et al. 2007; Hatch and Maibach 1995). Therefore, a complete and efficient removal of dye compounds from the water bodies is a greater need for the existing treatment plants to revive clean and edible water (Yagub et al. 2014).

Mordant Orange-1 (MO1) dye is an azo dye having complex aromatic structure and is highly stable in nature. It is synthesized by the diazo coupling reaction and these compounds are not degraded efficiently with the conventional waste water treatment plants (Abdel-Messih et al. 2013). Therefore, several methods are assessed for the removal of MO1 *viz*., adsorption (Li et al. 2018; Salama 2017), coagulation

(Shi et al. 2007; Li et al. 2016; Kuppusamy et al. 2017), foam separation (Schwarze et al. 2017), biological treatment etc. (Paz et al. 2017; Shen et al. 2018). However the existing water treatment plants showed additional environmental burden because it releases large amounts of sludge (Gracia-Lor et al. 2012). However, the commonly used chemical oxidants viz., chlorine, hypochlorite and ozone are widely employed because of their easy availability, cost effectiveness and possible efficiency. Although the use of these oxidants is based on the 'no waste' process it causes, in cases, the formation of harmful by-products or sometimes inadequate efficiency in particular towards the calcitrant chemicals. Moreover, the chlorination and ozonation are accompanied with formation of harmful disinfection by-products (DBPs) *viz*., hypohalous compounds (Krasner et al. 2009). These by-products are potential mutagens or carcinogens and are even more harmful compared to the parent compounds.

On the other hand, the advanced oxidation process (AOPs) using heterogeneous TiO_2 photocatalysis is highly efficient and relatively greener treatment processes to be employed in the waste water treatments. The principle of AOPs lies in the *in situ* formation of reactive hydroxyl radicals which readily oxidizes even persistent compounds in aqueous wastes. Further, widespread use of TiO_2 as the heterogeneous catalyst is because of its unique properties *viz*., excellent thermal and chemical stability, biocompatibility, low toxicity, low cost, easy fabrication, engineered material etc. However the bare titanium dioxide possessed a wide band gap energy and showed a rapid charge recombination rate which restricted its implications in the treatment processes. Therefore, alternatively the doping of titanium dioxide with non-metal, transition metal or noble metal reduces significantly the band gap energy which allows readily to absorb visible light (Mogal et al. 2014). The doped titanium dioxide shows an enhanced reactivity in the photocatalytic process using the visible light or even to harness the solar radiations (Ge et al. 2006). The noble metals (Ag, Au, Pd and Pt) show unusually high Schottky barriers which help trapping of electrons and reduced electron-hole pairs recombination. They also exhibit surface plasmon resonance (SPR) effect which enables titanium dioxide catalysts to absorb light at the visible region and enhances the excitation of electrons and enhances the photocatalytic efficiency (Selvaraj and Li 2006) (Zangeneh et al. 2015). Silver (Ag) nanoparticles show enormously intense surface plasmon resonance (SPR) effect at the wavelength of 320–450 nm near the band gap energy of titanium dioxide (~3.2 eV, 388 nm). In Ag^0 TiO_2 photocatalyst, movement of electrons between the conduction band of titanium dioxide and Ag nanoparticles is favourable since Fermi level of silver metal is lower as compared to the titanium dioxide (Selvaraj and Li 2006). This causes the generation of Schottky barriers within the metal-semiconductor which helps excited electrons to move toward the electric field and the holes toward the opposite direction of the electric field. This inhibits the fast electron-hole pair recombination (Liu et al. 2013; Lee et al. 2006). Therefore, the Ag^0(NP)/TiO_2 is a promising photocatalyst for variety of photocatalytic reactions (Z et al. 2014; Sofianos et al. 2014; Tiwari et al. 2018, 2020). The doping of noble metal nanoparticles within the TiO_2 network often leads to the agglomeration which greatly affects the catalytic action. Therefore, the communication deals with a suitable template synthesis of titanium dioxide with *in situ* and facile doping of Ag^0(NP) to the titanium dioxide crystal structure. Moreover, thin film of Ag^0(NPs)/ TiO_2 (nanocomposite) was obtained by the simple dip coating process. The insight of the catalytic activity of

thin film was conducted in the elimination of Mordant Orange-1 in aqueous wastes using UV-A and LED light illuminations.

Materials And Methods

Chemicals used

$Ti[OCH(CH_3)_2]_4$ (97.0%), $AgSO_4$, CH_3COOH, $NaBH_4$, polyethylene glycol (PEG) and Mordant Orange-1 are the product of Sigma Aldrich. Co., USA. Ethylene diamine tetraacetate (98.0%) and glacial acetic acid are obtained from Loba Chemicals, India. Ethanol (anhydrous) (99.9%) is procured from Changshu Yangyuan Chemicals, China. NaCl (99.0%), NaN_3 (99.0%), oxalic acid dihydrate (99.0%), 2-propanol (99.7%), $NiCl_2$ (95.0%), $CuSO_4$ (99.0%), glycine (99.9%) and $NaNO_3$ are product of Merck India Ltd., India. Purified water is collected from Sartorius water Purification System (model: Arium Mini Plus UV Lab., Sterile Plus, Sartopore 2150, Germany; Pore Size of 0.45 + 0.2 mm). Real water sample is obtained from Reiek Kai site of Tlawng river, near Aizawl city (India). Analytical results of the river water sample are given in Table 2. Spectrophotometer (UV-1800, Shimadzu, Japan) is employed for measuring the absorbance data of MO1.

Standard MO1 (50.0 mg/L) solution is prepared carefully in distilled water. Using this MO1 solution is diluted to obtain various concentrations of MO1 viz., 0.5, 1.0, 5.0, 10.0, 15.0 and 20.0 mg/L and utilized for obtaining the calibration line. The λ_{max} 371.5 nm is obtained for MO1. The degradation kinetics of MO1 was conducted obtaining the concentrations of MO1 at various time intervals. The TOC (Shimadzu, Japan; Model: TOC-VCPH/CPN) Analyser is used analysing apparent mineralization of MO1.

Methodology

The Ag^0(NP) are obtained by simple reduction process (Rashid et al.; Lalliansanga et al. 2019a). Further, the nanocomposite Ag^0(NPs)/TiO_2 is obtained by a facile sol gel synthetic route and the thin films are fabricated as described in detail elsewhere (Tiwari et al. 2018, 2020).

Characterization of the thin film

Ag^0(NPs)/TiO_2 thin film is analysed using SEM (Model: FE-SEM SU-70, Hitachi, Japan) images. Further, high resolution structural images are obtained using the TEM (Tecnai F20 Transmission Electron Microscope, FEI, USA) analyser. AFM (XE-100 apparatus from Park Systems, Korea) gives the 3D topographical images of nanocomposite thin films.

Reactor operation in the degradation of Mordant Orange-1

The concentration dependent studies are conducted by differing the initial concentrations of MO1 from 0.5 to 20.0 mg/L and pH is adjusted using 1.0 mol/L HCl/NaOH. The photocatalytic elimination of MO1 is performed in a self-assembled black box. The pollutant solution (50 mL) is taken inside the black box.

Nanocomposite thin film is taken inside the reactor vessel. UV-A illumination having λ_{max} of 360 nm (Model: 9 W, PLS9 W BLB/2 P 1CT, Philips) or a visible LED light (Havells- Adore LED 20 W, India) was placed *Ca* 12 cm above to dye solution. This provides the light-radiation passes through the dye solution and reaches to the thin film photocatalyst surface. This leads to initiate the photocatalytic degradation of MO1 at thin film surface. Self-assembled water keeps the reactor temperature (24±1 °C). The treated solution of MO1 is analysed by UV-Vis spectrophotometer at certain time intervals maximum up to 2 hr of photo-illumination. Further, the blank experiment is conducted to use only UV-A or LED light illuminations in absence of thin film photocatalyst.

Results And Discussion

Characterization of thin film

SEM micrographs of Ag^0(NP)/TiO_2 are shown in Figure 1(a). The result showed that small sized TiO_2 particles are distributed uniformly onto the silicate glass and formed a uniform thin film of nanocomposite. However, at places the cracks are observed onto the surface. Further, it is interesting to observe that the titanium dioxide is not agglomerated on the surface. This is because of the template synthesis to titania. The EDX analysis of the thin film sample was conducted and shown in Figure 1(a) (Inset). It is evident from the figure that the silver is incorporated within the titania network. Similarly, the TEM image of the nanocomposite is shown in Figure 1(b). The high resolution TEM image clearly showed the fringes of Ag nanoparticles and it is uniformly distributed with TiO_2 structure. Moreover, the interplanar distance of the Ag^0(NP) is estimated as 0.15 nm.

Similarly, the AFM image of nanocomposite thin film is shown as in Figure 1(c). AFM image inferred that the surface of thin film of photocatalystis highly uneven or heterogeneous in nature and the surface is possessed with small-sized pillars of titanium dioxide having maximum height of *Ca*. 350 nm. Further, the root mean square roughness (R_q) and mean roughness (R_a) of thin film is 16.952 nm and 12.250 nm, respectively.

Photocatalytic removal of MO1

pH dependence removal

Effect of pH is an useful parameter that demonstrates the mechanism of photocatalytic elimination of pollutants. This is mainly due to the pH dependence transitions in pollutant species as well as the surface properties of active sites of photocatalysts (Lalhriatpuia et al. 2015). Therefore, the pH influenced the overall efficiency of the photocatalyst in the degradation of pollutant molecules (Zucca et al. 2008). Photocatalytic elimination of MO1is carried out for a wide range of pH (4.0-10.0) and results are depicted as in Figure 2. The percentage removal of the MO1 was obtained after the 2 hr irradiation. Results clearly showed that the decrease in pH i.e., pH 10.0 to 4.0 has caused to increase the elimination of MO1. Quantitatively, with an decrease in solution pH from 10.0 to 4.0, the corresponding increase in percent

removal of MO1 is from 29.15 to 61.3% (for UV-A) and 16.65 to 35.81% (for LED light) using nanocomposite thin film photocatalyst. The MO1 molecule contains two dissociable hydrogens one from the carboxylic group and second is due to the phenolic group which are having the pk_a values of 5.0 and 11.0 (Nazar et al. 2010).Therefore, within the pH region 6.0-10.0, the MO1 molecule usually exists as mono-anionic species. However, the phenolic and carboxylic groups forming the hydrogen bonding resulting a non-ionic species. Hence, in this pH range the MO1 molecule exists in equilibrium between the the mono-anionic species (*Cf* Figure 2 (Inset)) (Nazar et al. 2010).Further,pH >10.0, both the protons of MO1 molecule are dissociated hence, the mono-anionic MO1 molecule becomes di-anionic species. Thus, the net charge of the MO1 species greatly becomes negative at and above pH 10.0. On the other hand, the pH_{pzc} of nanocomposite was obtained to be 6.8 (Tiwari et al. 2020). This infers that the thin film possesses net positive charge pH <6.8 whereas its surface possesses negative charges pH >6.8. These studies showed that increasing the pH gradually enhances the net negative charges both on the nanocomposite surface and MO1 species. This eventually caused an enhanced coulombic repulsions between the MO1 species and nanocomposite surface which resulted in gradual decrease of MO1 removal at pH>6.0 (pH 6~10). Photocatalytic removal of Alizarin Yellow using the catalyst Au^0(NPs)/TiO_2 thin film showed similar trends (Lalliansanga et al. 2019b). Further, reaction was conducted employing UV-A and LED illuminations without using nanocomposite thin films at a wide range of pH (pH 4.0-10.0). It was observed that a negligible amount of MO1 molecules was degraded after 2 hr of contact. These results clearly inferred that the nanocomposite catalyst greatly favoured the elimination of MO1 in aqueous media by UV-A or LED lights. Further, compared to the UV-A and LED light illumination, the UV-A light showed relatively higher degradation of MO1 throughout the studied pH.

Concentration dependence removal of MO1

Concentration dependence elimination of MO1 is analysed for varied concentration of MO1 (0.5 - 20.0 mg/L; pH 6.0). Removal efficiency of MO1 is illustrated in figure 3. Figure 3 demonstrates that decrease in concentration greatly favoured removal efficiency of MO1. Decreasing concentration of MO1 from 20.0 to 0.5 mg/L had enabled to increase the percentage degradation of MO1 from 13.7 to 60.6% (for UV-A) and 6.5 to 38.14% (LED light), respectively. The decrease in degradation efficiency with an increase in concentration of MO1 is, perhaps, due to the reason that the contact possibility of MO1 at the photocatalyst surface was relatively less at higher concentration of MO1 dye (Tiwari et al. 2015). It is also evident that at high concentration of MO1, the scavenging effect increases which possibly results in decrease of percentage removal of the MO1 (Nasseri et al. 2017).Furthermore, dark reaction is performed employing the catalyst Ag^0(NPs)/TiO_2 at various concentrations of MO1 (0.5–20.0 mg/L; pH 6.0). It was observed that almost negligible amount of MO1 was removed even after 12 hr of contact. Therefore, this indicates that no surface adsorption is taking place using the nanocomposite thin film for at least for MO1.

Kinetic study of MO1 degradation

The time dependence kinetics is carried out to assess the performance of nanocomposite photocatalyst in the elimination of MO1.The kinetic results are at varied concentrations of MO1 is shown in Table 1. It is observed that degradation of MO1 is proceeds through pseudo-first-order rate equation (Lalliansanga et al. 2019b). Further, the time dependent degradation kinetics of MO1 is favoured with the dilution i.e., increasing the concentration of the dyes result in decrease in the rate constant values. Moreover, the rate of degradation of MO1 is faster using the UV-A light irradiations compared to the LED light irradiations. Similar data is reported earlier where methylene blue was degraded using graphene decorated TiO_2 (Acosta-Esparza et al. 2020).

Table 1 Pseudo-first order rate constants in the photo-catalytic removal of MO1 employing nanocomposite thin film employing under UV-A and LED light irradiations [pH of solution: 6.0].

Initial Concentration of MO1 (mg/L)	UV-A Irradiation		LED Light Irradiation	
	Rate constant k_1x10^{-3}	R^2	Rate Constant k_1x10^{-3}	R^2
0.5	7.0	0.965	4.1	0.998
1.0	5.9	0.993	3.4	0.982
5.0	4.0	0.987	2.5	0.999
10.0	2.9	0.9895	1.8	0.998
15.0	2.0	0.979	1.1	0.995
20.0	1.4	0.952	0.5	0.994

Additionally, the removal of MO1 is modelled to the Langmuir–Hinshelwood (L-H) rate kinetics using the standard equations (Lalliansanga et al. 2019b). Therefore, the Langmuir–Hinshelwood (L-H) adsorption constant (k_r;mg/L/min) and the reaction rate constant (K; L/mg) are computed as 0.038 and 0.202 (R^2: 0.997 for UV-A) and 0.018 and 0.255 (R^2: 0.976 for LED), respectively.

Mineralization of MO1

Theextent of mineralization of pollutants in the photocatalytic treatment demonstrates the efficiency of operation. The percentage mineralization of MO1 is obtained at a wide range of concentration (1.0 to 20.0 mg/L; pH~6.0). Results are shown as in Figure 4(a). Results indicated that decrease in concentration of MO1 from 20.0 to 1.0mg/L had caused to increase the percentage mineralization of MO1 from 7.72 to 27.38% (for UV-A light) and from 4.12 to 17.1% (for LED light), respectively. The single reactor operation enabled to mineralize significantly the percentage mineralization of MO1. The finding are similar to the concentration dependent studies conducted previously in the removal of MO1. On the other hand, the photolysis using the UV-A or LED irradiation

showed almost negligible degradation of MO1. Therefore, the photocatalytic operations favoured the mineralization of MO1 using the nanocomposite thin film photocatalyst (Tiwari et al. 2015).

Repetitive use of thin film photocatalyst

The efficiency of the photocatalyst largely depends on its reusability for successive reactor operations. Therefore, the reusability of nanocomposite thin film photocatalyst is carried out for repeated reactor operations in the elimination of MO1 (MO1 concentration: 5.0 mg/L; pH 6.0). The percentage elimination of MO1 with effect of number of cycles of reactor operations are shown as in Figure 4(b). The degradation efficiency of the photocatalyst is almost unaffected even at the end of six successive cycles of reactor operations,. Quantitatively, the percentage degradation of MO1 is decreased only from 40.29% to 40.23% (i.e., 0.06%). The results showed that thin film catalyst is reasonably stable towards the reactor operations in photocatalytic degradation of MO1. Hence, the photocatalyst is shown to be employed for prolonged and sustainable operations.

Simultaneous presence of co-ions

Applicability of thin film catalyst is further assessed in presence of variety of co-ions *viz.,* glycine, oxalic acid, $NaNO_3$, NaCl, $CuSO_4$, $NiCl_2$ and EDTA. The initial concentration of MO1 and co-existing ions was taken to be 5.0 mg/L and 50.0 mg/L, respectively (pH 6.0 and UV-A illumination for 2h). The removal efficiency of MO1 for simultaneous presence of co-ions is shown in Figure 5(a). The removal efficiency of MO1 is affected to by the NaCl, EDTA and glycine. However, the other ions introduced have not affected significantly the degradation of MO1 in the photocatalytic reactor operations.

Degradation mechanism

It is known that the photons carrying enough energy (hυ) may generate electron and hole pairs (Selvaraj and Li 2006). However, titanium dioxide possessed wide band gap energy (3.2 eV) hence, excited by the photons at UV region only. However, the doping of titanium dioxide by noble metals (Ag or Au) lowers apparent band gap energy. Noble metal nanoparticles generates a phenomenon called localised surface plasmon resonance which enables TiO_2 photocatalyst to absorb light within the visible region and enhances the photo-excitation of electrons (Zangeneh et al. 2015). It also traps the newly generated electrons thus helping in reducing the charge recombination rate and allow it to proceed further for photocatalytic reaction. Therefore, in order to demonstrate the possible mechanism involved in the elimination of MO1 using the nanocomposite photocatalyst, the investigation was extended in presence of several scavengers.2-propanol and HCO_3^- compounds are known $^{\bullet}OH$ radical scavengers (Xu et al. 2015; Lalhriatpuia et al. 2016); whereas EDTA scavenges the h^+ of photocatalyst (Jia et al. 2016). Similarly, the sodium azide traps singlet oxygen which are generated in reaction of $O_2^{-\bullet}$ with h^+ (Xu et al. 2015). Thus, the degradation of MO1 (5.0 mg/L; pH 6.0) in presence of these scavengers is carried out using the UV-A irradiation for 2h. The degradation efficiency of MO1 is shown as in Figure 6(b). The results inferred that the 2-propanol, HCO_3^- and sodium azide are greatly hampered the percentage

degradation of MO1. This indicated that hydroxyl radicals are primarily involved in the degradation process. Additionally, NaN_3 suppressed the removal efficiency of MO1, inferred that singlet oxygen is taking part in photocatalytic degradation reaction. Hence, it infers that the elimination mechanism of MO1 proceeds in two different possible pathways. First, the Ag(NPs) traps the newly generated electrons which helps in inhibiting the charge recombination and allow it to go further for reaction to form peroxide radical and hydroxyl radicals (Ahmad et al. 2016). Peroxide radicals are generated at the conduction band through interaction of trapped electrons and oxygen in presence of water while hydroxyl radicals are generated at the valence band through the interaction of the H_2O and oxygen (Akpan and Hameed 2009). Both the radicals then interacted with the pollutant on the vicinity of the thin film photocatalyst which results in the degradation of MO1 (Vogna et al. 2004; Tiwari et al. 2019). The other possible pathway is that Ag(NPs) absorbs light radiations resulting the generation of electromagnetic field as because of localized surface plasmon resonance (Lee et al. 2014). Further, Schottky barrier present with metal-semiconductor causes the excited electrons to move toward the electric field and the holes towards the opposite direction of the electric field. This inhibits the recombination of electron-hole pairs (Z et al. 2014). Further, the electron-hole pairs undergo further reaction to form peroxide radical and hydroxyl radical which take part in the degradation of MO1.

Real water treatment

Applicability of fabricated Nano catalyst depends greatly on its utility to real water samples. Hence, intended performance of Nano catalyst thin film in the elimination of MO1 was performed using the MO1 tagged real water samples. Previously, physico/chemical parameters are obtained for this water and shown is Table 2. The real water contained high concentrations of Fe, Ca and Zn. On the other hand, the TOC data showed that real water is contained with high inorganic carbon value with less NPOC value. MO1 was tagged with real water having various concentrations of MO1 (0.5 to 20.0 mg/L; pH 6.0). Further, degradative removal of MO1 is carried out using nanocomposite thin film catalyst under UV-A and LED light illuminations for 2h. Percentage degradation of MO1 was obtained and compared with the result obtained with the purified water samples (*Cf* Figure 6). The study revealed that the percentage degradation of MO1 is not significantly decreased in real water samples. This signifies the high applicability of nanocomposite thin film catalyst in the removal of MO1.

Table 2 Various Physico-chemical Parametric Analysis of Reiek Kai Site, Tlawng River Water.

Parameters Studied	Analytical Results
pH	7.6
Conductivity	0.0172 S/m
Resistivity	0.0138 Mohm.cm
Salinity	0.12 PSU
Ox. Red. Potential	210.7 mV
Elements studied (AAS)	**(mg/L)**
Ni	0.0
Zn	0.535
Pb	0.078
Mn	0.01
Fe	0.198
Ca	2.341
Cu	0.0
TOC Analysis	**(mg/L)**
Inorganic Carbon	13.94
NPOC	2.493
Anions studied	**(mg/L)**
Nitrate	11.43
Fluoride	0.0
Sulphate	6.12
Phosphate	0.09

Conclusion

Nanocomposite (Ag^0(NPs)/TiO_2) is obtained using the facile template process. The thin film catalyst was fabricated by the dip coating process. SEM images showed Ag is successfully doped uniformly within the titania network and the interplanar distance of Ag^0(NPs) was 0.15 nm. AFM analysis showed that nanocomposite forming a heterogeneous structure on the glass substrate. The root mean square roughness (Rq) and mean roughness (Ra) of catalyst was 16.952nm and 12.250nm, respectively. Thin film catalyst was utilized for the elimination of Mordant Orange-1 using UV-A and LED light irradiations. Lower pH values and lower concentrations of MO1 have favoured greatly the removal efficiency of MO1.

Increase in MO1 concentration from 0.5–20.0 mg/L had caused to decrease the percentage removal of MO1 from 60.61–13.74% and 38.14–6.5% under UV-A and LED irradiation, respectively. Photocatalytic elimination of MO1 has proceeded through pseudo-first order rate kinetics. Moreover, partial but significantly the MO1 was mineralized by a single operation indicated greater applicability of photocatalytic process. Increase in MO1 concentration from 1.0 to 20.0 mg/L the percentage mineralization of MO1 was seemingly lowered from 27.38–7.72% (for UV-A light) and from 17.1–4.12% (for LED light), respectively. Further, the presence of NaCl, EDTA and glycine greatly influenced the degradation efficacy of the thin films. However, the other ions were not significantly affected the removal efficiency of MO1. The scavenger studies indicated that the degradation of MO1 is primarily due to the reactive hydroxyl radicals, holes and singlet oxygen which are primarily involved in the surface excitations. Moreover, the repetitive use of thin film catalyst showed almost no suppression in photocatalytic efficiency of thin film hence, the nanocomposite thin films possesses greater applicability in sustained reactor operations. Additionally, the real matrix operations using the Reiek Kai site, Tlawng river, Aizawl (India) water showed almost similar removal efficiency compared to the distilled water treatment.

Declarations

Ethical approval: Not applicable

Consent to participate: Not Applicable

Consent to publish: Not Applicable

Funding: No funding to report

Competing interests: The authors declare that they have no competing interests.

Availability of data and materials: No Applicable

Author Contributions: C.V.L.H. (Ph.D. Student) conducted the basic experiments relating to the photocatalytic reactor operations. C.L. (Asst. Professor) fabricated the thin film samples and helped in compiling the data. D.T. (Professor) has formulated the problem and finalized the manuscript. D.J.K. (Professor) has helped in drafting the paper and made corrections in the final paper.

References

1. Abdel-Messih MF, Ahmed MA, El-Sayed AS (2013) Photocatalytic decolorization of Rhodamine B dye using novel mesoporous SnO2–TiO2 nano mixed oxides prepared by sol–gel method. J Photochem Photobiol Chem 260:1–8. https://doi.org/10.1016/j.jphotochem.2013.03.011
2. Acosta-Esparza MA, Rivera LP, Pérez-Centeno A et al (2020) UV and Visible light photodegradation of methylene blue with graphene decorated titanium dioxide. Mater Res Express 7:035504.

https://doi.org/10.1088/2053-1591/ab7ac5

3. Ahmad R, Ahmad Z, Khan A et al (2016) Photocatalytic Systems as an Advanced Environmental Remediation: Recent Developments, Limitations and new Avenues for Applications. J Environ Chem Eng 4:4143–4164. https://doi.org/10.1016/j.jece.2016.09.009
4. Akpan UG, Hameed BH (2009) Parameters affecting the photocatalytic degradation of dyes using TiO2-based photocatalysts: a review. J Hazard Mater 170:520–529. https://doi.org/10.1016/j.jhazmat.2009.05.039
5. Alves de Lima RO, Bazo AP, Salvadori DMF et al (2007) Mutagenic and carcinogenic potential of a textile azo dye processing plant effluent that impacts a drinking water source. Mutat Res 626:53–60. https://doi.org/10.1016/j.mrgentox.2006.08.002
6. Ge L, Xu M, Fang H (2006) Preparation and characterization of silver and indium vanadate co-doped TiO2 thin films as visible-light-activated photocatalyst. J Sol-Gel Sci Technol 40:65–73. https://doi.org/10.1007/s10971-006-8457-9
7. Gracia-Lor E, Sancho JV, Serrano R, Hernández F (2012) Occurrence and removal of pharmaceuticals in wastewater treatment plants at the Spanish Mediterranean area of Valencia. Chemosphere 87:453–462. https://doi.org/10.1016/j.chemosphere.2011.12.025
8. Gupta VK, Suhas (2009) Application of low-cost adsorbents for dye removal – A review. J Environ Manage 90:2313–2342. https://doi.org/10.1016/j.jenvman.2008.11.017
9. H K, M S-N, S M-D HS (2017) Enhanced photocatalytic degradation of dyes over graphene/Pd/TiO_2 nanocomposites: TiO_2 nanowires versus TiO_2 nanoparticles. J Colloid Interface Sci 498:423–432. https://doi.org/10.1016/j.jcis.2017.03.078
10. Hai F, Yamamoto K, Fukushi K (2007) Hybrid treatment systems for dye wastewater. Fac Sci - Pap Arch. https://doi.org/10.1080/10643380601174723
11. Hatch KL, Maibach HI (1995) Textile dye dermatitis. J Am Acad Dermatol 32:631–639. https://doi.org/10.1016/0190-9622(95)90350-x
12. Husain Q (2006) Potential applications of the oxidoreductive enzymes in the decolorization and detoxification of textile and other synthetic dyes from polluted water: a review. Crit Rev Biotechnol 26:201–221. https://doi.org/10.1080/07388550600969936
13. Jia Y, Liu J, Cha S et al (2016) Magnetically separable Au-TiO2/nanocube ZnFe2O4 composite for chlortetracycline removal in wastewater under visible light. J Ind Eng Chem 47:. https://doi.org/10.1016/j.jiec.2016.12.001
14. Jin X-C, Liu G-Q, Xu Z-H, Tao W-Y (2007) Decolorization of a dye industry effluent by Aspergillus fumigatus XC6. Appl Microbiol Biotechnol 74:239–243. https://doi.org/10.1007/s00253-006-0658-1
15. Jung K-W, Choi BH, Hwang M-J et al (2016) Fabrication of granular activated carbons derived from spent coffee grounds by entrapment in calcium alginate beads for adsorption of acid orange 7 and methylene blue. Bioresour Technol 219:185–195. https://doi.org/10.1016/j.biortech.2016.07.098

16. Krasner SW, Westerhoff P, Chen B et al (2009) Occurrence of disinfection byproducts in United States wastewater treatment plant effluents. Environ Sci Technol 43:8320–8325. https://doi.org/10.1021/es901611m
17. Kuppusamy S, Kadiyala V, Palanisami T et al (2017) Quercus robur acorn peel as a novel coagulating adsorbent for cationic dye removal from aquatic ecosystems. Ecol Eng 101:3–8. https://doi.org/10.1016/j.ecoleng.2017.01.014
18. Lalhriatpuia C, Tiwari A, Shukla A et al (2016) Nanopillars TiO2 thin film photocatalyst application in the remediation of aquatic environment. Korean J Chem Eng 33:3367–3373. https://doi.org/10.1007/s11814-016-0191-6
19. Lalhriatpuia C, Tiwari D, Tiwari A, Lee S-M (2015) Immobilized Nanopillars-TiO2 in the efficient removal of micro-pollutants from aqueous solutions: Physico-chemical studies. Chem Eng J 281:782–792. https://doi.org/10.1016/j.cej.2015.07.032
20. Lalliansanga TD, Tiwari A et al (2019a) Facile synthesis and characterization of nanocomposite Au0(NPs)/titanium dioxide: Photocatalytic degradation of Alizarin Yellow. J Ind Eng Chem 82:. https://doi.org/10.1016/j.jiec.2019.10.008
21. Lalliansanga TD, Tiwari A et al (2019b) Facile synthesis and characterization of nanocomposite Au0(NPs)/titanium dioxide: Photocatalytic degradation of Alizarin Yellow. J Ind Eng Chem 82:. https://doi.org/10.1016/j.jiec.2019.10.008
22. Lee H, Lee YK, Hwang E, Park JY (2014) Enhanced surface plasmon effect of Ag/TiO2 nanodiodes on internal photoemission. J Phys Chem C 118:5650–5656. https://doi.org/10.1021/jp409894b
23. Lee YH, Matthews RD, Pavlostathis SG (2006) Biological decolorization of reactive anthraquinone and phthalocyanine dyes under various oxidation-reduction conditions. Water Environ Res Res Publ Water Environ Fed 78:156–169. https://doi.org/10.2175/106143005x89616
24. Li C, Lou T, Yan X et al (2018) Fabrication of pure chitosan nanofibrous membranes as effective absorbent for dye removal. Int J Biol Macromol 106:768–774. https://doi.org/10.1016/j.ijbiomac.2017.08.072
25. Li H, Liu S, Zhao J, Feng N (2016) Removal of reactive dyes from wastewater assisted with kaolin clay by magnesium hydroxide coagulation process. A Physicochemical and engineering aspects
26. Liu C, Lei Z, Yang Y et al (2013) Improvement in settleability and dewaterability of waste activated sludge by solar photocatalytic treatment in Ag/TiO2-coated glass tubular reactor. Bioresour Technol 137:57–62. https://doi.org/10.1016/j.biortech.2013.03.071
27. Matouq M, Al-Anber Z, Susumu N et al (2014) The kinetic of dyes degradation resulted from food industry in wastewater using high frequency of ultrasound. Sep Purif Technol C:42–47. https://doi.org/10.1016/j.seppur.2014.08.002
28. Mogal S, Gandhi G, Mishra M et al (2014) Single-Step Synthesis of Silver-Doped Titanium Dioxide: Influence of Silver on Structural, Textural, and Photocatalytic Properties. Ind Eng Chem Res 53:5749–5758. https://doi.org/10.1021/ie404230q

29. Muhd Julkapli N, Bagheri S, Bee Abd Hamid S (2014) Recent Advances in Heterogeneous Photocatalytic Decolorization of Synthetic Dyes. Sci World J 2014:e692307. https://doi.org/10.1155/2014/692307
30. Nasseri S, Mahvi AH, Seyedsalehi M et al (2017) Degradation kinetics of tetracycline in aqueous solutions using peroxydisulfate activated by ultrasound irradiation: Effect of radical scavenger and water matrix. J Mol Liq 241:704–714. https://doi.org/10.1016/j.molliq.2017.05.137
31. Nazar MF, Shah SS, Khosa MA (2010) Interaction of Azo Dye with Cationic Surfactant Under Different pH Conditions. J Surfactants Deterg 13:529–537. https://doi.org/10.1007/s11743-009-1177-8
32. Papić S, Koprivanac N, Božić AL, Meteš A (2004) Removal of some reactive dyes from synthetic wastewater by combined Al(III) coagulation/carbon adsorption process. Dyes Pigments 3:291–298. https://doi.org/10.1016/S0143-7208(03)00148-7
33. Paz A, Carballo J, Pérez MJ, Domínguez JM (2017) Biological treatment of model dyes and textile wastewaters. Chemosphere 181:168–177. https://doi.org/10.1016/j.chemosphere.2017.04.046
34. Rashid MU, Bhuiyan MKH, Quayum ME Synthesis of Silver Nano Particles (Ag-NPs) and their uses for Quantitative Analysis of Vitamin C Tablets. Dhaka Univ J Pharm Sci 12:29
35. Riera-Torres M, Gutiérrez-Bouzán C, Crespi M (2010) Combination of coagulation–flocculation and nanofiltration techniques for dye removal and water reuse in textile effluents. Desalination 252:53–59. https://doi.org/10.1016/j.desal.2009.11.002
36. Rosu M-C, Coros M, Pogacean F et al (2017) Azo dyes degradation using TiO2-Pt/graphene oxide and TiO2-Pt/reduced graphene oxide photocatalysts under UV and natural sunlight irradiation. Solid State Sci 70:13–20. https://doi.org/10.1016/j.solidstatesciences.2017.05.013
37. Sadeghzade-Attar A (2018) Efficient photocatalytic degradation of methylene blue dye by SnO2 nanotubes synthesized at different calcination temperatures. Sol Energy Mater Sol Cells 183:16–24. https://doi.org/10.1016/j.solmat.2018.03.046
38. Salama A (2017) New sustainable hybrid material as adsorbent for dye removal from aqueous solutions. J Colloid Interface Sci 487:348–353. https://doi.org/10.1016/j.jcis.2016.10.034
39. Schwarze M, Gross M, Ebraheme A A, et al (2017) Biopolymers for Dye Removal via Foam Separation. Sep Purif Technol 188:. https://doi.org/10.1016/j.seppur.2017.07.025
40. Selvaraj R, Li X (2006) Enhanced Photocatalytic Activity of TiO2 by Doping with Ag for Degradation of 2,4,6-Trichlorophenol in Aqueous Suspension. J Mol Catal Chem 243:. https://doi.org/10.1016/j.molcata.2005.08.010
41. Shen L, Jin Z, Wang D et al (2018) Enhance wastewater biological treatment through the bacteria induced graphene oxide hydrogel. Chemosphere 190:201–210. https://doi.org/10.1016/j.chemosphere.2017.09.105
42. Shi B, Li G, Wang D et al (2007) Removal of direct dyes by coagulation: the performance of preformed polymeric aluminum species. J Hazard Mater 143:567–574. https://doi.org/10.1016/j.jhazmat.2006.09.076

43. Sofianos MV, Boukos N, Vaimakis T, Trapalis C (2014) Decoration of TiO2 anatase nanoplates with silver nanoparticles on the {1 0 1} crystal facets and their photocatalytic behaviour. Appl Catal B Environ s 158–159:91–95. https://doi.org/10.1016/j.apcatb.2014.02.030
44. Su C-C, Pukdee-Asa M, Ratanatamskul C, Lu M-C (2011) Effect of operating parameters on decolorization and COD removal of three reactive dyes by Fenton's reagent using fluidized-bed reactor. Desalination 278:211–218. https://doi.org/10.1016/j.desal.2011.05.022
45. Tiwari A, Shukla A, Lalliansanga et al (2019) Au-nanoparticle/nanopillars TiO2 meso-porous thin films in the degradation of tetracycline using UV-A light. J Ind Eng Chem 69:141–152. https://doi.org/10.1016/j.jiec.2018.09.027
46. Tiwari A, Shukla A, Lalliansanga null et al (2018) Nanocomposite thin films Ag0(NP)/TiO2 in the efficient removal of micro-pollutants from aqueous solutions: A case study of tetracycline and sulfamethoxazole removal. J Environ Manage 220:96–108. https://doi.org/10.1016/j.jenvman.2018.05.019
47. Tiwari A, Shukla A, Lalliansanga null et al (2020) Synthesis and characterization of Ag0(NPs)/TiO2 nanocomposite: insight studies of triclosan removal from aqueous solutions. Environ Technol 41:3500–3514. https://doi.org/10.1080/09593330.2019.1615127
48. Tiwari D, Lalhriatpuia C, Lalhmunsiama L et al (2015) Efficient application of nano-TiO2 thin films in the photocatalytic removal of Alizarin Yellow from aqueous solutions. Appl Surf Sci 353:275–283. https://doi.org/10.1016/j.apsusc.2015.06.131
49. Verma AK, Dash RR, Bhunia P (2012) A review on chemical coagulation/flocculation technologies for removal of colour from textile wastewaters. J Environ Manage 93:154–168. https://doi.org/10.1016/j.jenvman.2011.09.012
50. Vogna D, Marotta R, Napolitano A et al (2004) Advanced oxidation of the pharmaceutical drug diclofenac with UV/H2O2 and ozone. Water Res 38:414–422. https://doi.org/10.1016/j.watres.2003.09.028
51. Xu D, Liu K, Shi W et al (2015) Ag-decorated K2Ta2O6 nanocomposite photocatalysts with enhanced visible-light-driven degradation activities of tetracycline (TC). Ceram Int 3 Part B:4444–4451. https://doi.org/10.1016/j.ceramint.2014.11.136
52. Yagub MT, Sen TK, Afroze S, Ang HM (2014) Dye and its removal from aqueous solution by adsorption: a review. Adv Colloid Interface Sci 209:172–184. https://doi.org/10.1016/j.cis.2014.04.002
53. Z C, S Z, H Q, et al (2014) Preparation of visible-light nano-photocatalysts through decoration of TiO2 by silver nanoparticles in inverse miniemulsions. J Colloid Interface Sci 435:51–58. https://doi.org/10.1016/j.jcis.2014.08.021
54. Zangeneh H, Zinatizadeh AAL, Habibi M et al (2015) Photocatalytic oxidation of organic dyes and pollutants in wastewater using different modified titanium dioxides: A comparative review. J Ind Eng Chem 26:1–36. https://doi.org/10.1016/j.jiec.2014.10.043

55. Zucca P, Vinci C, Sollai F et al (2008) Degradation of Alizarin Red S under mild experimental conditions by immobilized 5,10,15,20-tetrakis(4-sulfonatophenyl)porphine–Mn(III) as a biomimetic peroxidase-like catalyst. J Mol Catal Chem 288:97–102. https://doi.org/10.1016/j.molcata.2008.04.001

Figures

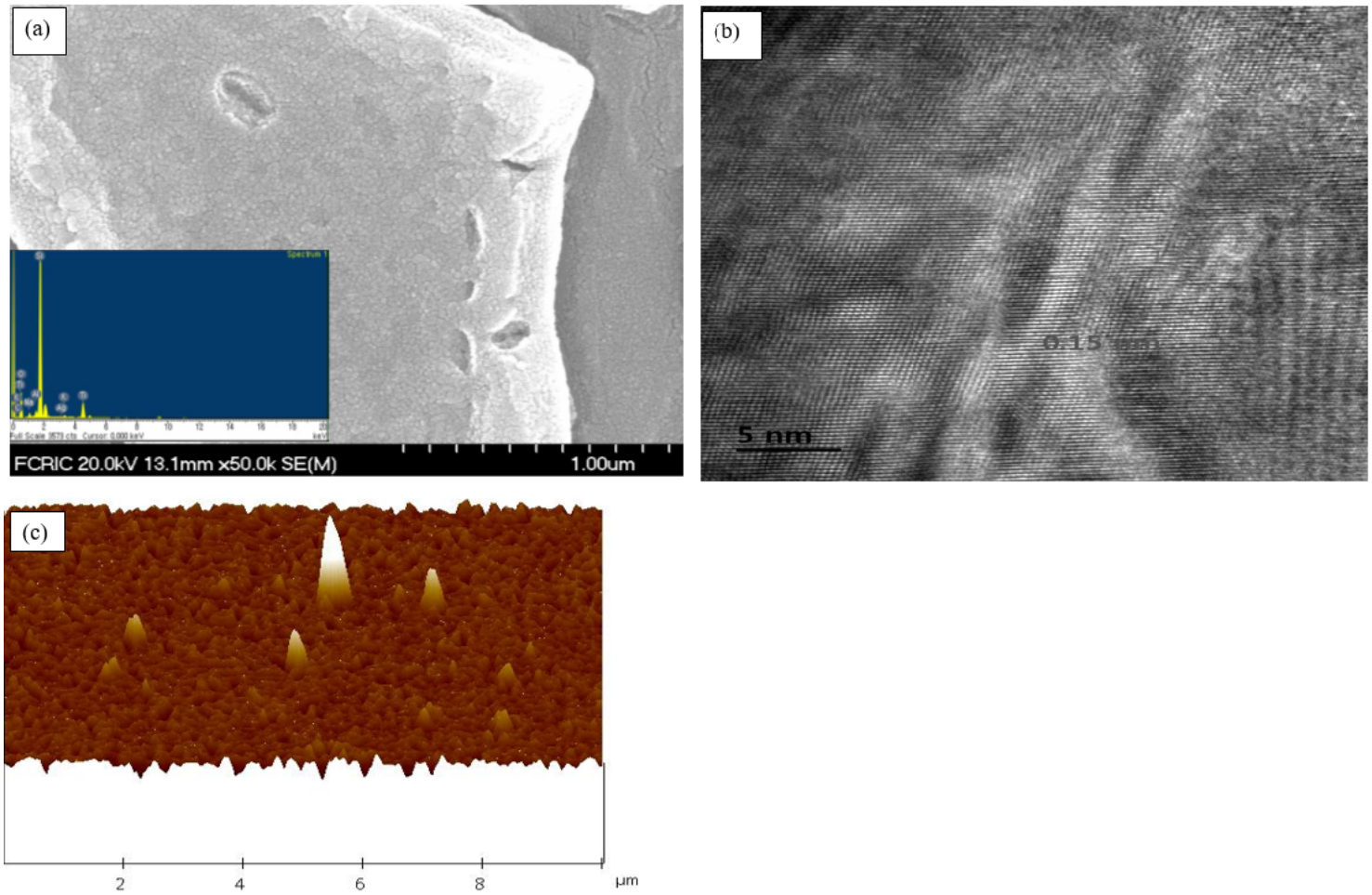

Figure 1

Morphological studies of the nanocomposite material (a) SEM image of thin film; (b) TEM image of the Ag0(NPs)/TiO2 nanocomposite and (c) AFM image of thin film (Scale X: 2 µm/div; Z: 350 µm/div and data scale 350 nm).

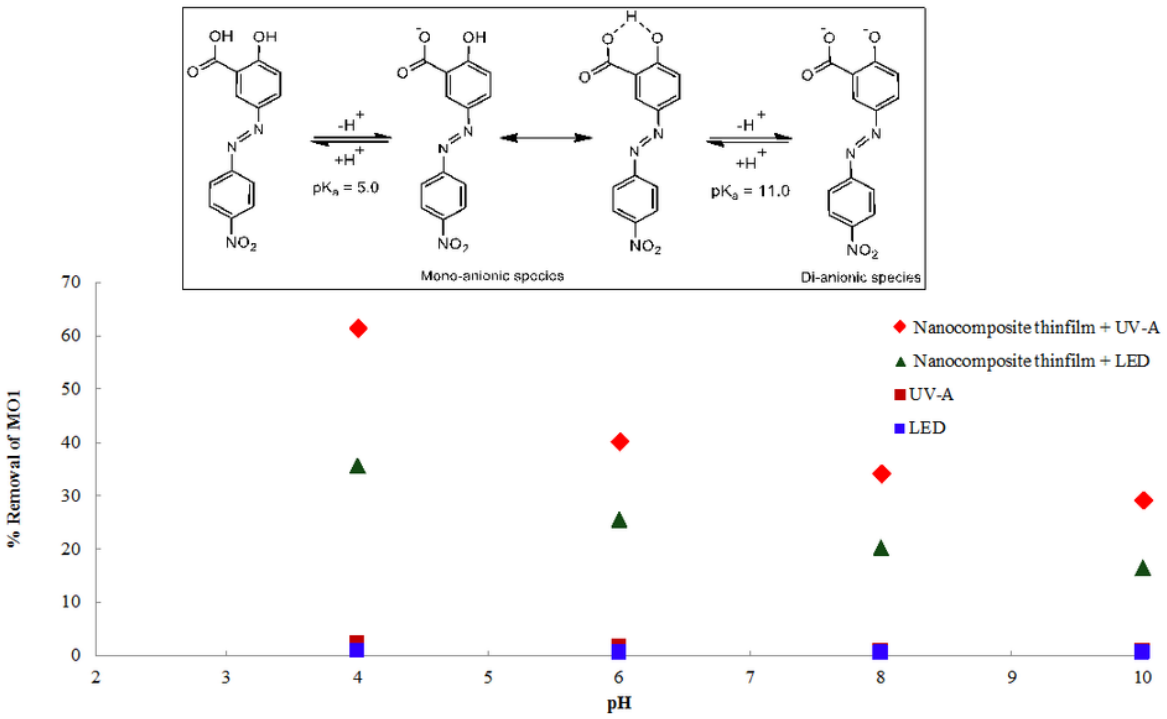

Figure 2

Percentage elimination of MO1 with effect of solution pH [Initial Concentration of MO1: 5.0 mg/L] and the Inset the Equilibrium of MO1 as function of pH.

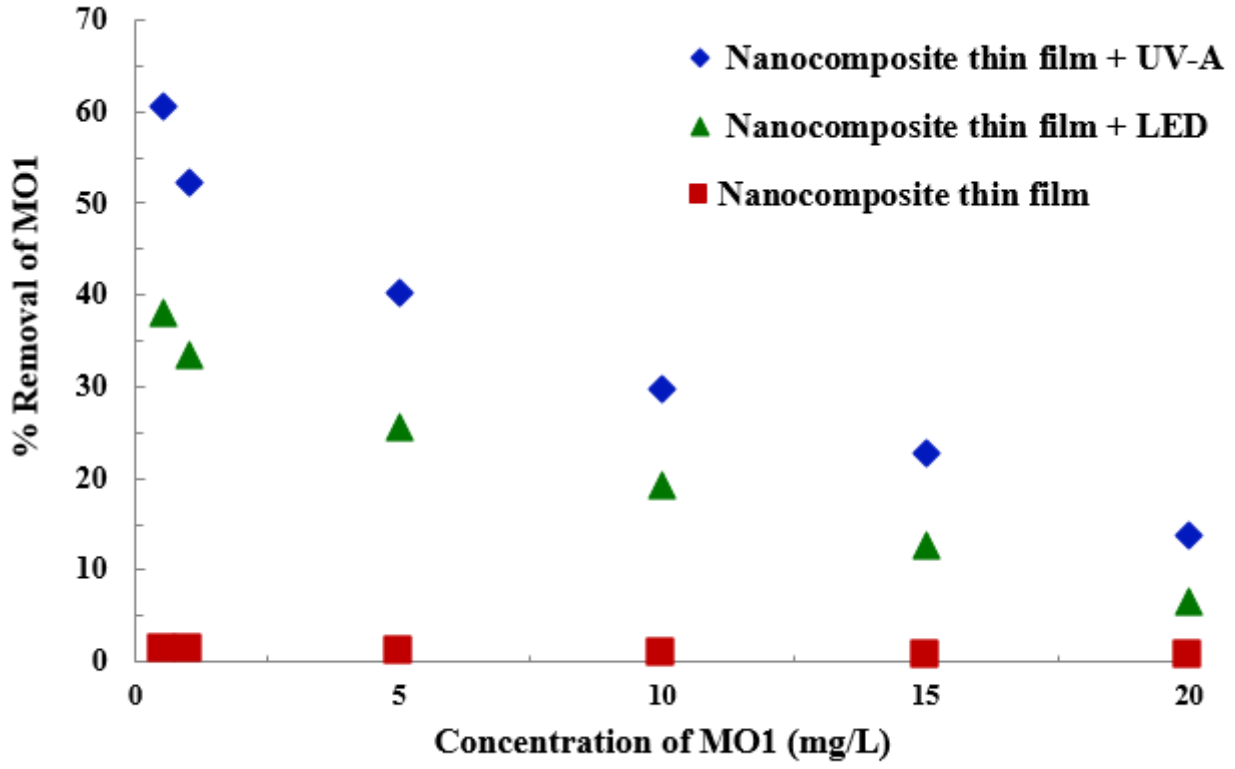

Figure 3

Removal efficiency of MO1 as function of concentration of MO1 [pH of solution: 6.0].

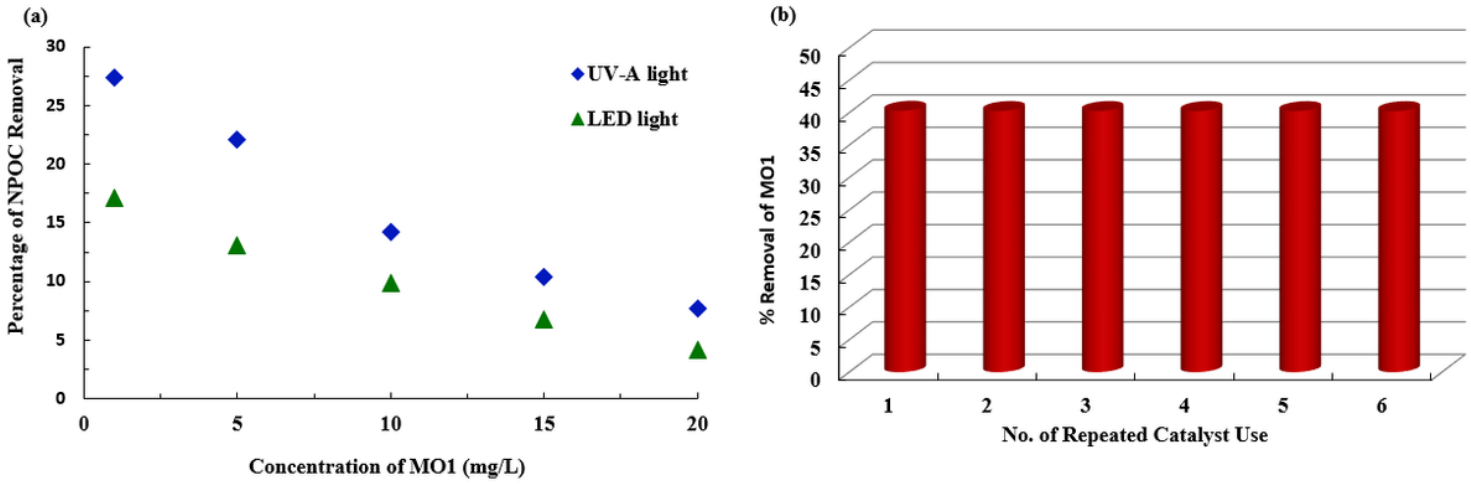

Figure 4

(a) Percentage mineralization of MO1 as a function of MO1 concentrations under the photocatalytic processes; and (b) elimination efficiency of MO1 after repeated cycle of catalyst operations [pH of solution: 6.0].

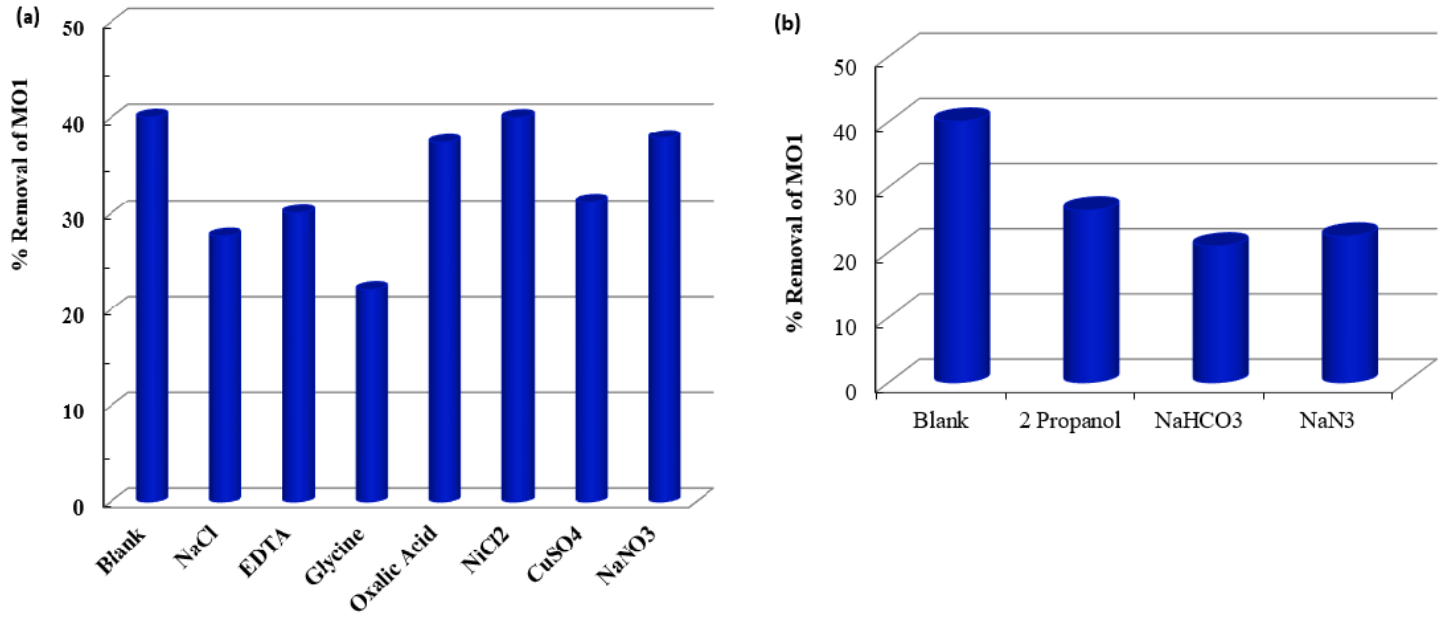

Figure 5

Photocatalytic elimination of MO1 with effect of (a) Several co-existing ions [Concentration of MO1: 5.0 mg/L; Concentration of Co-existing ions: 50.0 mg/L; pH:6.0] and (b) several scavengers [Concentration of MO1: 5.0 mg/L; Concentration of scavengers: 500.0 mg/L; pH:6.0].

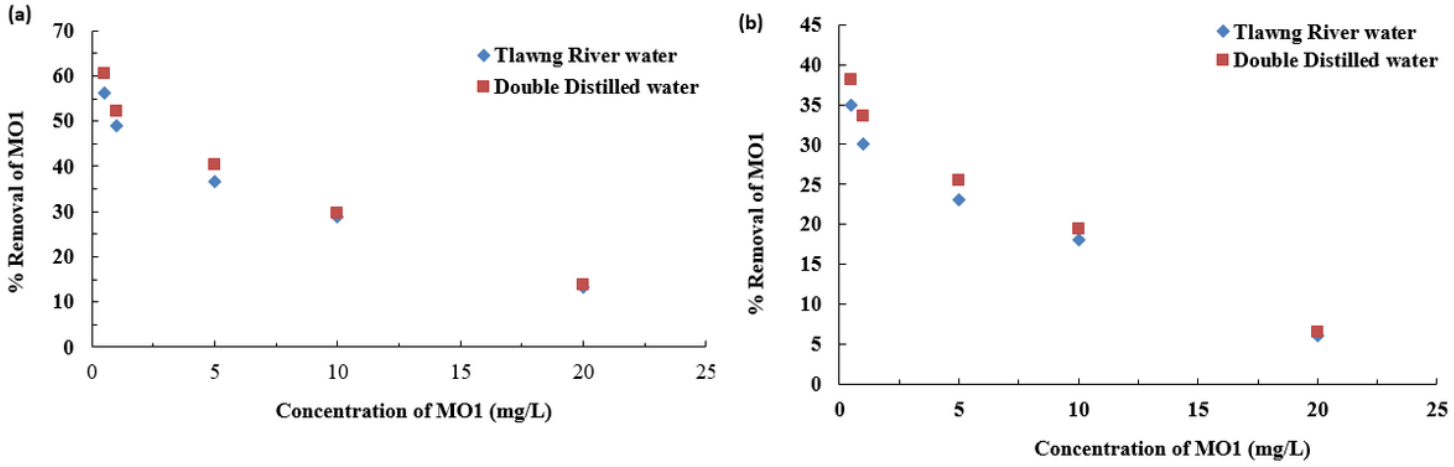

Figure 6

Photocatalytic elimination of MO1 in distilled water and Tlawng river water using the nanocomposite thin film catalyst under (a) UV-A and (b) LED light